Sedimentology (2003) **50,** 247–263

Threshold for particle entrainment into suspension

YARKO NIÑO*, FABIAN LOPEZ† and MARCELO GARCIA‡
**Department of Civil Engineering, University of Chile, Avenida Blanco Encalada 2002, Santiago, Chile (E-mail: ynino@cec.uchile.cl)*
†Instituto Nacional del Agua y del Ambiente, Avenida Ambrosio Olmos 1142, 5000 – Córdoba, Argentina
‡Department of Civil and Environmental Engineering, University of Illinois at Urbana-Champaign, 205 N. Mathews, Urbana, IL 61801, USA

ABSTRACT

Laboratory observations regarding the limit conditions for particle entrainment into suspension are presented. A high-speed video system was used to investigate conditions for the entrainment of sediment particles and glass beads lying over a smooth boundary as well as over a rough bed. The results extend experimental conditions of previous studies towards finer particle sizes. A criterion for the limit of entrainment into suspension is proposed which is a function of the ratio between the flow shear velocity and particle settling velocity. Observations indicate that particles totally immersed within the viscous sublayer can be entrained into suspension by the flow, which contradicts the conclusions of previous researchers. A theoretical analysis of the entrainment process within the viscous sublayer, based on force–balance considerations, is used to show that this phenomenon is related to turbulent flow events of high instantaneous values of the Reynolds stress, in agreement with previous observations. In the case of experiments with a rough bed, a hiding effect was observed, which tends to preclude the entrainment of particles finer than the roughness elements. This implies that, as the ratio between particle and roughness element sizes becomes smaller, progressively higher bed shear stresses are required to entrain particles into suspension. On the other hand, an overexposure effect was also observed, which indicates that a particle moving on a smooth bed is more prone to be entrained than the same particle moving on a bed formed by identical particles.

Keywords Entrainment, sediment, suspension, turbulence.

INTRODUCTION

The concept of a threshold bed shear stress for the initiation of motion of a sediment particle lying in a bed of similar particles has long occupied a central position in sediment transport theory (e.g. DuBoys, 1879; Shields, 1936). Nevertheless, Grass (1970) and, later, Lavelle & Mofjeld (1987) criticized the concept and proposed, based on empirical evidence such as that by Grass (1971), an alternative statistical view of particle movement on the bed. Turbulent fluctuations in instantaneous bottom shear stress and the random exposure of bed grains to the flow make it possible for particles to move, even at very low values of the mean bed shear stress. From this point of view, the definition of a threshold condition for the initiation of motion appears to have only statistical significance, although it may still maintain its convenience in practice.

A similar argument can be used to address the definition of the threshold conditions for the entrainment of particles into suspension. However, the definition of a limit for particle entrainment into suspension can also have practical convenience, for instance in distinguishing regimes of sediment transport such as bedload and suspended load (García, 2000), or to know under what conditions contaminated sediment might be resuspended (López & García, 2001).

Different criteria and theories have been developed to define a threshold condition for particle entrainment into suspension. In all these, the turbulence of the flow is assumed to have a major influence on the phenomenon. Indeed, the problem of particle entrainment into suspension has been related to turbulence–particle interactions taking place in the near-bed region of the flow (e.g. Sutherland, 1967; Grass, 1974; Sumer & Oguz, 1978; Yung *et al.*, 1988; Rashidi *et al.*, 1990; Williams *et al.*, 1994; Kaftori *et al.*, 1995a; Niño & García, 1996; Niño & Musalem, 2000). According to these studies, particles are lifted from the bed and entrained into suspension under the action of coherent flow structures related to the turbulent bursting process (Robinson, 1991).

Bagnold (1966) proposed one of the first criteria to estimate the threshold condition for particle entrainment. This was based on the assumption that particles remain in suspension as long as the turbulent eddies have dominant vertical velocity components, which would scale with the flow shear velocity, u^*, that exceed the particle settling velocity, w_s. Accordingly, the critical value of the flow shear velocity for the initiation of suspension would satisfy the condition: $u^*/w_s = 1$. Previously, Engelund (1965a,b) proposed two different criteria to estimate the threshold conditions for the initiation of suspension. These criteria, which were also expressed in terms of the ratio u^*/w_s, with values of 0·25 and 0·85, respectively, have been discussed by Niño (1995) and Niño & García (1998a).

More recently, van Rijn (1984) conducted a series of experiments to determine the limit conditions for the initiation of suspension. Although he did not give enough details about the experiments, it seems that they correspond to observations of particle entrainment from a mobile bed formed by similar particles. van Rijn (1984) presented his results in the form of a range of limit conditions for which sediment particles are lifted from the bed into suspension. The analysis of these results together with the condition proposed by Bagnold (1966) is presented below.

In this paper, experimental results regarding the threshold conditions for particle entrainment into suspension are presented and discussed on the basis of a theoretical analysis of this phenomenon. The entrainment of particles lying over a smooth boundary as well as over a rough bed is investigated, including the phenomenon of hiding associated with the motion of particles with sizes smaller than that of the roughness elements of the bed.

PRELIMINARY CONSIDERATIONS

Consider a fully turbulent open channel flow with a bed formed by granular material of small size compared with the flow depth. A typical dimensionless relation characterizing the limiting conditions for the entrainment of bed particles into bedload motion can be written as (Raudkivi, 1990):

$$f_1(Re_p*,\ \tau*) = 0 \qquad (1)$$

where $Re_p^* = u^* d_p/\nu$ denotes a particle Reynolds number, with u^* denoting the flow shear velocity, d_p denoting a representative mean diameter of the entrained particles, and ν denoting the kinematic viscosity of the fluid; also, $\tau^* = u^{*2}/(gRd_p)$ denotes a dimensionless bed shear stress (i.e. Shields' stress), with g denoting gravitational acceleration, $R = (\rho_s - \rho)/\rho$ denoting the submerged specific density, and ρ_s and ρ denoting the density of the entrained particle and the density of the fluid respectively.

It can be argued that Eq. 1 can also be used to represent a dimensionless relation characterizing the limit of entrainment into suspension of particles lying over the granular bed of the open channel flow. In fact, u^* is a measure of the turbulence intensity of the flow in the near-bed region, therefore τ^* can be interpreted as a measure of the ratio of turbulent lift to gravitational force acting on the particle. On the other hand, Re_p^* is a measure of the relative size of the particle with respect to the thickness of the viscous sublayer. Clearly, particles with larger values of both τ^* and Re_p^* are more prone to be entrained into suspension than those with lower values of these parameters.

For the particular case in which the size of the entrained particle is different from the size of the particles forming the roughness elements of the bed, d_b, one more parameter must be included in a relation such as Eq. 1. This takes the form of a ratio d_p/d_b, which quantifies effects such as hiding, when this ratio is <1·0, and overexposure, when this ratio is >1·0.

In this case, Eq. 1 becomes:

$$f_2(R_p,\ \tau^*,\ d_p/d_b) = 0 \qquad (2)$$

where the parameter Re_p^* has been replaced by the parameter $R_p = (Rgd_p^3)^{1/2}/\nu$, which is a kind of dimensionless particle diameter that depends on the properties of the particle and the fluid, but is independent of flow parameters. These

two parameters are related by the transformation:

$$Re_p^* = R_p \tau^{*1/2} \quad (3)$$

In fact, van Rijn (1984) uses a relation equivalent to Eq. 2 to plot his experimental results on the threshold for particle entrainment into suspension (with $d_p/d_b = 1$), although van Rijn expresses it in terms of a dimensionless parameter D^* instead of R_p, such that $D^* = R_p^{2/3}$.

Another alternative dimensionless relationship for the limit of entrainment can be written as:

$$f_3(R_p,\ u*/w_s,\ d_p/d_b) = 0 \quad (4)$$

As w_s is related to the particle size, the ratio u^*/w_s is equivalent to τ^*, and can be interpreted as a measure of the ratio between turbulent lift and forces that oppose particle motion, such as gravitational and viscous forces acting over the particle. In fact, Bagnold's (1966) criterion for particle entrainment into suspension mentioned previously is expressed in terms of a relation equivalent to Eq. 4.

EXPERIMENTAL STUDY

The experiments were conducted in a rectangular open channel, 18·6 m long and 0·30 m wide, with a slope set to a value of about 0·0009. The channel has an observation window located 12 m downstream from the entrance. A high-speed video system, the Kodak Ektapro TR motion analyser, was used to record particle motion. A strobe light with a flash duration of 20 μs was synchronized with the high-speed video system to provide whole-field illumination and to reduce image blur resulting from particle motion.

The experiments were carried out under uniform flow conditions. Particles were fed externally to the flow at a distance sufficiently far upstream from the observation window (about 6 m) to ensure that particle motion reached independence from initial conditions before going into the field of view of the camera. The amount of particles fed to the flow and their distribution over the bottom wall were controlled to create a uniform single-size layer of particles, with a surface coverage of about 15–20%. Particle motion was recorded from the side through the observation window, using the high-speed video system set at a recording rate of 250 frames per second.

Different particle sizes were analysed. For each particle size, the experimental conditions were initially set so that the particles would move close to the channel bottom, as bedload only. After recording particle motion for a few minutes, the flow rate was increased in order to increase the flow depth and thus the bed shear stress. The video recording of particle motion was then repeated only after reaching uniform flow conditions. This procedure was continued until conditions of generalized particle transport in suspension were obtained.

Two different series of experiments (S and T) were conducted corresponding to two different surface roughness conditions. The first series of experiments (Series S) corresponded to a channel with smooth walls. The second series (Series T) corresponded to a channel with bottom roughness in the transitionally rough regime. The bottom roughness in this case was of the k-type (Perry & Li, 1990), that is it was created by gluing sand particles, with a mean size $d_b = 530$ μm, to the originally smooth surface of the channel bottom.

Flow depths used in both series of experiments covered a range from about 25 mm to about 70 mm. Water temperature was in the range from 19·5 to 20·5 °C, and fluid kinematic viscosity was estimated as $\nu = 1 \times 10^{-6}$ m^2 s^{-1}. Flow conditions corresponded to values of the flow Reynolds number (defined as $Re = Uh/\nu$, where U denotes flow mean velocity, and h denotes flow depth) in the range from about 5000 to about 35000, and to values of the Froude number [defined as $Fr = U/\sqrt{(gh)}$] of about 0·5–0·6, which corresponded to subcritical flows. Values of u^*, estimated for each experimental condition by means of a best fit of velocity measurements made at the channel centreline with a hot-film probe to the logarithmic velocity distribution (Niño, 1995), were in the range from about 0·015 m s^{-1} to about 0·040 m s^{-1}.

Five different types of particles, with uniform size distributions, were used in the Series S and T experiments, namely glass beads with mean diameter, d_p, of 38 and 94 μm, and natural silica sand particles with d_p values of 112, 224 and 530 μm respectively. Values of d_p correspond to the median size d_{50}. All the particles had a value of $R = 1{\cdot}65$. Values of the dimensionless parameter R_p were in the range from 0·9 to 50. For the present range of values of particle diameter and shear velocity, resulting values of the dimensionless shear stress, τ^*, were in the range from 0·03 to 2, whereas the values of Re_p^* ranged from 0·6 to 20. In some of the experiments in Series S,

particles had sizes smaller than the corresponding thickness of the viscous sublayer (estimated as $5\nu/u^*$). In the experiments in Series T, where the size of the particles transported by the flow, d_p, was different from the size of the particles forming the roughness elements of the bed, d_b, the ratio d_p/d_b had values in the range from 0·07 to 1·0. A summary of the particle characteristics used in the present experimental study is shown in Table 1, including associated values of the settling velocity estimated using:

$$w_S = \left(\frac{4}{3}\frac{Rgd_p}{c_D}\right)^{1/2} \tag{5}$$

which is valid for spherical particles, and where c_D denotes the drag coefficient estimated from (Yen, 1992):

$$c_D = \frac{24}{Re_p}(1 + 0{\cdot}15Re_p^{1/2} + 0{\cdot}017Re_p) - \frac{0{\cdot}208}{1 + 10^4 Re_p^{-1/2}} \tag{6}$$

with $Re_p = w_s d_p/\nu$, this expression being valid over the whole range of values of Re_p in the present experiments.

EXPERIMENTAL RESULTS

The video recordings of particle motion were analysed by two independent researchers to define the regime of sediment transport prevalent in each particular experiment. In general, the onset of particle suspension was more or less abrupt. For low values of the bed shear stress, the particles moved in contact with the bed. In the case of smooth flows, the particles moved along the bed only by rolling and sliding. In the case of transitionally rough flows, the particles moved mainly in saltation, except for those with small ratios d_p/d_b, which moved within the interstices of the much larger roughness elements of the bed. As the shear stress was increased, progressively more frequent events occurred, during which particles were suddenly entrained into the outer regions of the wall layer and remained in suspension for distances generally longer than 100 particle diameters. During these events, the particles clearly responded to large velocity fluctuations in the flow, of the kind associated with the turbulent bursting phenomenon (Robinson, 1991). Detailed descriptions of such responses, including measurements of particle and fluid velocities during entrainment events, and a full discussion of the nature of the interaction between particles and turbulence in these experiments have been reported elsewhere (Niño & García, 1996). The most frequent kind of coherent structure observed to cause particle entrainment into suspension corresponds to shear layers, described by García *et al.* (1995), which are related to flow ejection events of the second quadrant (see also Liu *et al.*, 1991; Urushihara *et al.*, 1993).

There appears to be a threshold level of bed shear stress for the particle to respond to turbulent ejections as defined by Niño & García (1996). Accordingly, a value of the threshold shear stress for suspension was defined for each particle size used in the present experiments, in terms of whether or not the particles responded to the turbulence and, in particular, to ejection events, as observed in the video recordings. A particle was considered to respond to ejections if, after entrainment, it remained in suspension for a distance longer than 100 particle diameters, according to a similar criterion defined by van Rijn (1984). Of course, the definition of the precise threshold level has only statistical significance. Actually, there is a transition range of increasing values of the shear stress in which the frequency of the entrainment events, and the number of particles entrained by those events, increases from a negligible value to a large value (Niño & García, 1996). Nevertheless, this range is, in practice, rather narrow, and a more precise definition of the threshold does not seem to be necessary.

A summary of the results obtained from the analysis described above is presented in Table 2. The results are also plotted in Figs 1 and 2, corresponding to the experiments in Series S and T, respectively, using the parameter space (Re_p^*, τ^*).

Table 1. Properties of the particles used in the experimental study.

d_p (μm)	w_s (cm s^{-1})	R_p	d_p/d_b
38	0·13	0·9	0·072
94	0·70	3·7	0·177
112	0·96	4·8	0·211
224	3·00	13·5	0·423
530	8·91	49·1	1·000

ENTRAINMENT FROM A SMOOTH BED

No particles in the experiments with $d_p = 530$ μm were suspended for the present range of shear

Table 2. Threshold conditions for particle entrainment into suspension.

Series	Expt	d_p (μm)	h (m)	U (m s^{-1})	u^* (m s^{-1})	R_p	Re_p^*	τ^*	Suspension
S1	S11	38	0·025	0·261	0·017	0·9	0·63	0·446	No
	S12	38	0·030	0·301	0·018	0·9	0·69	0·534	No
	S13	38	0·035	0·336	0·019	0·9	0·74	0·622	No
	S14	38	0·040	0·372	0·021	0·9	0·79	0·710	No
	S15	38	0·045	0·409	0·022	0·9	0·84	0·798	Yes
	S16	38	0·050	0·448	0·023	0·9	0·89	0·886	Yes
S2	S21	94	0·025	0·261	0·017	3·7	1·56	0·180	No
	S22	94	0·030	0·299	0·018	3·7	1·70	0·216	No
	S23	94	0·035	0·338	0·020	3·7	1·84	0·252	Yes
	S24	94	0·040	0·373	0·021	3·7	1·96	0·287	Yes
	S25	94	0·045	0·410	0·022	3·7	2·08	0·323	Yes
	S26	94	0·050	0·444	0·023	3·7	2·19	0·358	Yes
S3	S31	112	0·025	0·260	0·017	4·8	1·85	0·151	No
	S32	112	0·030	0·300	0·018	4·8	2·03	0·181	Yes
	S33	112	0·035	0·338	0·020	4·8	2·19	0·211	Yes
	S34	112	0·040	0·375	0·021	4·8	2·34	0·241	Yes
	S35	112	0·045	0·410	0·022	4·8	2·48	0·271	Yes
	S36	112	0·050	0·444	0·023	4·8	2·61	0·301	Yes
S4	S41	224	0·025	0·261	0·017	13·5	3·71	0·076	No
	S42	224	0·030	0·300	0·018	13·5	4·06	0·091	No
	S43	224	0·035	0·338	0·020	13·5	4·38	0·106	Yes
	S44	224	0·040	0·375	0·021	13·5	4·68	0·120	Yes
	S45	224	0·045	0·410	0·022	13·5	4·96	0·135	Yes
	S46	224	0·050	0·446	0·023	13·5	5·23	0·150	Yes
S5	S51	530	0·025	0·261	0·017	49·1	8·78	0·032	No
	S52	530	0·030	0·300	0·018	49·1	9·61	0·038	No
	S53	530	0·035	0·338	0·020	49·1	10·37	0·045	No
	S54	530	0·040	0·375	0·021	49·1	11·08	0·051	No
	S55	530	0·045	0·410	0·022	49·1	11·74	0·057	No
	S56	530	0·050	0·445	0·023	49·1	12·37	0·064	No
T1	T11	38	0·043	0·370	0·028	0·9	1·08	1·258	No
	T12	38	0·053	0·428	0·033	0·9	1·25	1·681	No
T2	T21	94	0·035	0·313	0·024	3·7	2·26	0·335	No
	T22	94	0·039	0·339	0·026	3·7	2·45	0·416	No
	T23	94	0·044	0·374	0·029	3·7	2·70	0·520	No
	T24	94	0·044	0·375	0·029	3·7	2·71	0·520	No
	T25	94	0·049	0·406	0·031	3·7	2·93	0·619	No
	T26	94	0·052	0·426	0·033	3·7	3·08	0·680	No
	T27	94	0·069	0·524	0·040	3·7	3·79	1·027	No
T3	T31	112	0·028	0·264	0·020	4·8	2·27	0·215	No
	T32	112	0·032	0·297	0·023	4·8	2·55	0·273	No
	T33	112	0·040	0·346	0·027	4·8	2·98	0·372	No
	T34	112	0·048	0·397	0·031	4·8	3·42	0·489	No
	T35	112	0·055	0·444	0·034	4·8	3·82	0·613	No
	T36	112	0·069	0·525	0·040	4·8	4·52	0·862	Yes
T4	T41	224	0·028	0·268	0·021	13·5	4·61	0·109	No
	T42	224	0·031	0·288	0·022	13·5	4·96	0·129	No
	T43	224	0·035	0·317	0·024	13·5	5·46	0·157	No
	T44	224	0·040	0·351	0·027	13·5	6·04	0·193	No
	T45	224	0·045	0·379	0·029	13·5	6·53	0·225	No
	T46	224	0·048	0·399	0·031	13·5	6·87	0·250	Yes
	T47	224	0·052	0·426	0·033	13·5	7·33	0·285	Yes
	T48	224	0·057	0·456	0·035	13·5	7·86	0·328	Yes
T5	T51	530	0·069	0·524	0·040	49·1	21·36	0·182	No

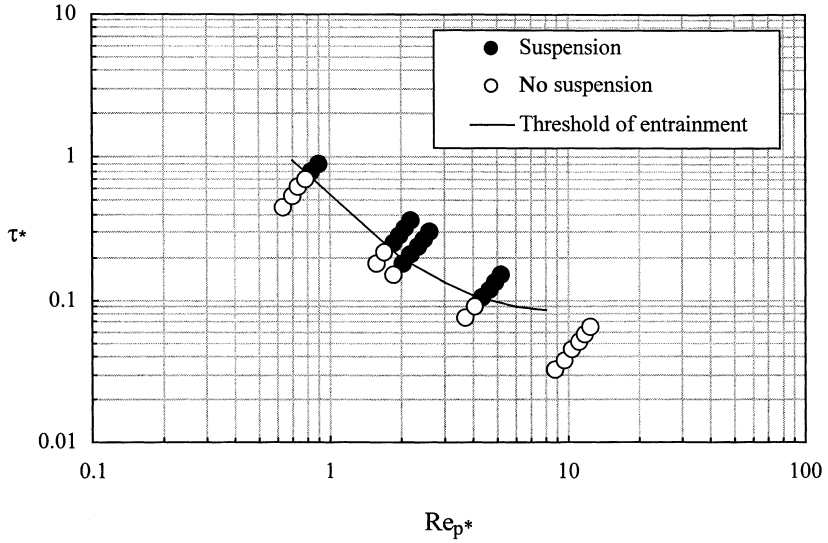

Fig. 1. Threshold of entrainment into suspension for Series S. Circles represent experimental conditions at which either entrainment or no entrainment was observed. The line shows the threshold of entrainment and was traced by eye.

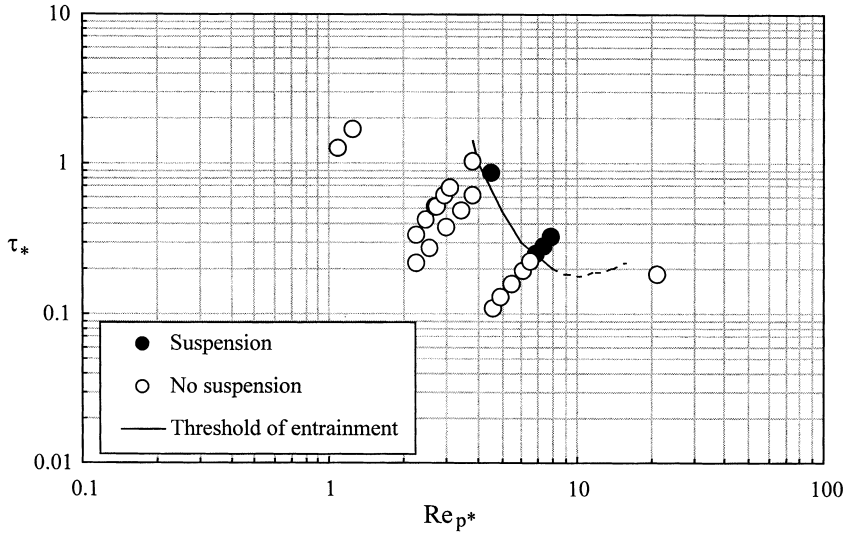

Fig. 2. Threshold of entrainment into suspension for Series T. Circles represent experimental conditions at which either entrainment or no entrainment was observed. The line represents the threshold of entrainment and was traced by eye.

stresses. In the case of smooth flows, such particles just moved along the bed by sliding and rolling, whereas in the case of transitionally rough flows, they moved by saltation, with increasingly higher and longer jumps for increasing values of bed shear stress (Niño & García, 1998b).

Experimental points corresponding to values of Re_p* lower than about 5 (Fig. 1) are associated with particle sizes smaller than the thickness of the viscous sublayer of the flow (this thickness corresponds approximately to a value $y^+ = yu^*/\nu = 5$, where y denotes the distance from the bed). According to the present observations, particles totally immersed in the viscous sublayer are entrained into suspension if the bed shear stress is sufficiently large, which contradicts previous observations by Sumer & Oguz (1978) and Yung *et al.* (1988) (see also Niño & García, 1996). Also, as the particle size decreases, progressively higher values of the dimensionless shear stress are required for entrainment. This is rather obvious, as the turbulence intensities of the flow surrounding the particle, which are responsible for lifting the particle into suspension, become relatively less strong as the particle becomes more and more immersed in the viscous sublayer (Nezu & Nakagawa, 1993; García *et al.*, 1995). A theoretical analysis of this phenomenon is presented in the next section.

A comparison of the present experimental values of the threshold of entrainment in smooth flows with the experimental results of van Rijn (1984) and also with the theoretical relationship

proposed by Bagnold (1966) is represented in Fig. 3, in the parameter space (R_p, τ^*). The classical Shields' curve for the limit of particle motion is also plotted in Fig. 3 as a reference, as given by the equation proposed by Brownlie (1981). Bagnold's (1966) criterion for the initiation of suspension, given by: $u^*/w_s = 1$, was plotted in Fig. 3 using the relation:

$$\tau^* = \frac{u*^2}{Rgd_p} = \frac{w_S^2}{Rgd_p} \tag{7}$$

According to van Rijn (1984), Bagnold's criterion defines an upper limit at which a concentration profile of suspended sediment starts to develop, whereas his limit of entrainment defines an intermediate stage at which locally turbulent bursts of sediment particles are lifted from the bed into suspension. In this sense, van Rijn's criterion for defining the limit of entrainment is equivalent to the one used in the present study. For values of R_p larger than about 8, the range proposed by van Rijn (1984) for the limit of entrainment agrees fairly well with the threshold curve resulting from present observations (Fig. 3). For lower values of this parameter, however, van Rijn's range tends to underestimate the present limit values of τ^* for which particles were entrained into suspension. Apparently, van Rijn did not conduct experiments in the range of values of R_p lower than about 8, but rather assumed that the limit of entrainment would approach the Shields' curve for very fine particles.

On the other hand, although Bagnold's criterion indeed overestimates the limit of entrainment obtained from present observations for values of R_p larger than about 10, Bagnold's limit of entrainment at lower values of R_p defines threshold values of τ^* that are too low compared with the present results. This is expected because Bagnold assumes that vertical velocity fluctuations of the flow, which must balance the settling velocity for the particle to be suspended, are of the order of u^*. This is true only at distances from the bed that are within the wall layer but at the same time outside the viscous sublayer as, inside the viscous sublayer, the vertical velocity fluctuations are dampened rather strongly as the bed is approached (Nakagawa & Nezu, 1981). Because of this, Bagnold's criterion is not applicable for values of $Re_p{}^*$ lower than about 5, or equivalently for values of R_p lower than about 10.

The experimental limit of suspension (Fig. 1) can also be expressed in terms of the ratio u^*/w_s (Fig. 4), as any given pair ($Re_p{}^*$, τ^*) can be transformed into a pair (R_p, u^*/w_s) using Eq. 3 together with Eq. 5. In Fig. 4, the experimental limit for the initiation of suspension proposed by van Rijn (1984), given by:

$$u^*/w_s = \begin{cases} 4{\cdot}0\,R_p^{-2/3} & 1 \le R_P \le 32 \\ 0{\cdot}4 & R_p \ge 32 \end{cases} \tag{8}$$

is also plotted together with Bagnold's (1966) criterion. Figure 4 shows tendencies similar to those discussed for Fig. 3; however, a comparison of the present results with Eq. 8 is not possible for values of R_p larger than about 50 because the present range of flow conditions did not allow entrainment of such large particles.

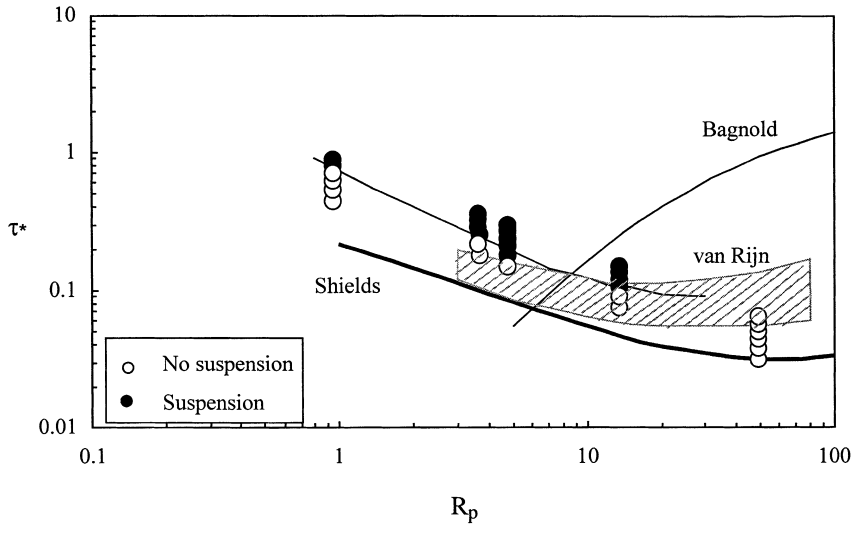

Fig. 3. Comparison between experimental results of Series S, Bagnold's (1966) threshold of entrainment criterion and Shields' curve. Also plotted is the region of threshold conditions for entrainment according to van Rijn (1984).

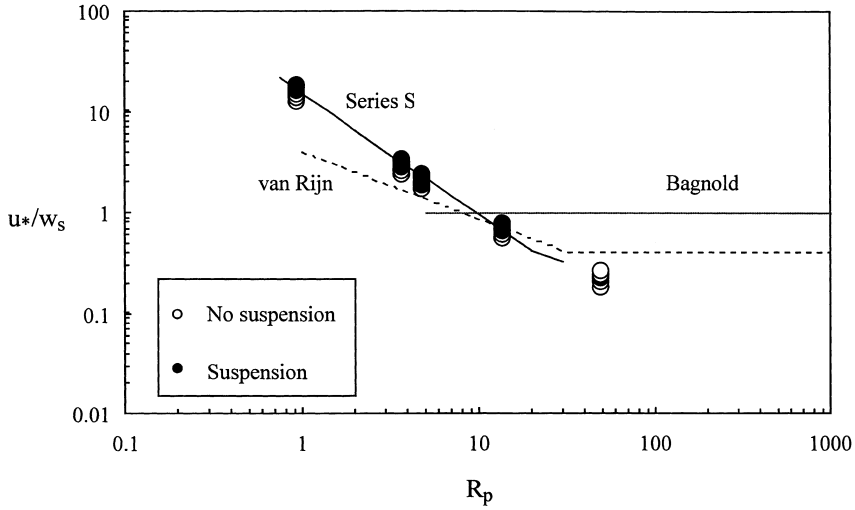

Fig. 4. Comparison between experimental results of Series S and the threshold of entrainment criteria proposed by Bagnold (1966) and van Rijn (1984).

A THEORY FOR ENTRAINMENT FROM A SMOOTH BED

A theoretical condition for particle entrainment can be expressed in terms of force–balance considerations. If W_s denotes the submerged weight of the sediment particles and F_t denotes the turbulent lift force acting over the particles, then the threshold condition for entrainment can be expressed as:

$$F_t = W_s \tag{9}$$

Considering spherical particles with mean diameter d_p, then $W_s = (\rho_s - \rho)g\pi d_p^3/6$. Two different approaches are explored to estimate F_t.

Mean lift force within the viscous sublayer

Mollinger & Nieuwstadt (1996) conducted a series of experiments to measure the mean lift force over spheres immersed within the viscous sublayer of a wall-bounded turbulent flow. They adjusted a model to their data, which is expressed as:

$$F_l = k\rho v^2/2^m Re_p{*}^m \tag{10}$$

where F_l denotes the mean lift force acting over a particle lying on the bottom wall, and k and m are constant coefficients with values of 56·9 and 1·87 respectively. Eq. 10 is valid in the range $0{\cdot}6 < Re_p{*} < 4$. Similar relationships have been proposed by Hall (1988), Leighton & Acrivos (1985) and Saffman (1965), and are valid for different ranges of $Re_p{*}$ values and have different values of k and m. These values and the range of validity corresponding to each of the above relationships are shown in Table 3.

Assuming that $F_t = F_l$, then Eq. 9 reduces to:

$$\tau^* = 4(\pi/6k)^{2/m} R_p^{2(2/m-1)} \tag{11}$$

which provides an equation to estimate the threshold dimensionless shear stress for entrainment as a function of the dimensionless particle diameter. A comparison of this relationship with the present experimental data is shown in Fig. 5 for the different values of k and m in Table 3.

Saffman's relationship seems to provide the best fit to the present experimental results (Fig. 5), although it is valid for values $Re_p{*} << 1$. On the other hand, Mollinger and Nieuwstadt's (1996) relationship, which should work best for the present experimental range of $Re_p{*}$, predicts that entrainment should occur for much lower values of the dimensionless shear stress than observed in the present experiments. It also predicts that the threshold dimensionless shear stress increases as R_p increases, in

Table 3. Values of coefficients k and m and range of validity of models for the mean lift force F_l.

Authors	k	m	Range of validity
Saffman (1965)	6·46	3·00	$Re_p{*} << 1$
Leighton & Acrivos (1985)	9·22	4·00	$Re_p{*} << 1$
Hall (1988)	20·90	2·31	$Re_p{*} > 6$
Mollinger & Nieuwstadt (1996)	56·90	1·87	$0{\cdot}6 < Re_p{*} < 4$

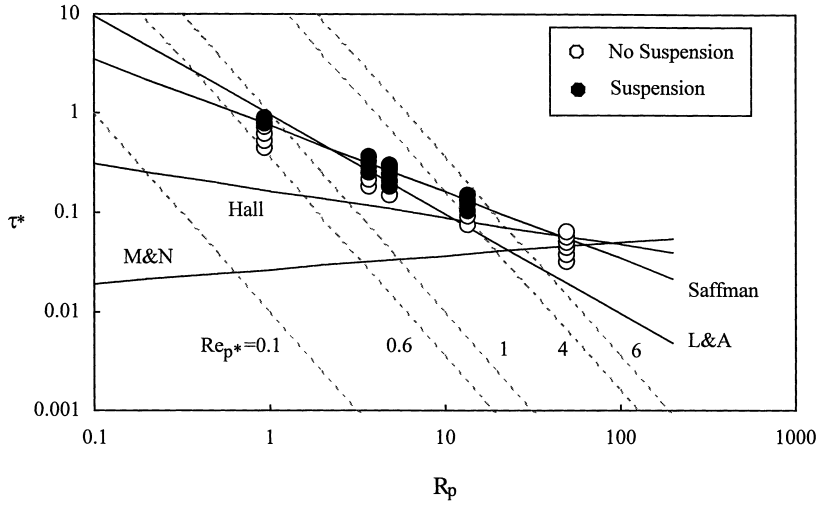

Fig. 5. Comparison between experimental results of Series S and theoretical predictions based on estimation of the mean lift force within the viscous sublayer. The solid lines represent different predictions obtained by using the models for the lift force proposed by Saffman (1965), Leighton & Acrivos (1985; L & A), Hall (1988) and Mollinger & Nieuwstadt (1996; M & N). The dashed lines represents curves of equal Re_p*.

opposition to the experimental observations (Fig. 5). These results suggest that the condition $F_t = F_l > W_s$ does not necessarily imply that the particle is going to be lifted away from the viscous sublayer. In other words, it appears that the mean lift force, F_l, acting over particles lying on the bed within the viscous sublayer of the flow is not large enough to cause their entrainment into suspension. Apparently, a force larger than that associated with the mean flow is required. This means that a different mechanism might be associated with particle entrainment rather than solely the lift forces associated with mean flow conditions. The following section adopts a different approach, in which the force responsible for entrainment, F_t, is estimated in terms of a turbulent velocity scale associated with flow events with large values of instantaneous shear stress.

Lift force associated with high instantaneous shear

It is assumed here that entrainment is caused by an intermittent force generated by a local, high instantaneous value of the Reynolds stress, such as those associated with the bursting process (Robinson, 1991). The force F_t is estimated using a drag formulation:

$$F_t = 1/2 C_D \rho u_e^2 \pi d_p^2/4 \qquad (12)$$

where u_e denotes a velocity scale associated with the entrainment. Using Eq. 5, it is easy to show that replacing Eq. 12 in Eq. 9 yields:

$$u_e/w_s = 1 \qquad (13)$$

which is basically Bagnold's condition for entrainment, although u_e needs to be correctly estimated. In order to estimate u_e, it is assumed that this velocity is related to the instantaneous Reynolds stress that is causing entrainment. The following relation is proposed:

$$u_e = \xi(\tau_p/\rho)^{1/2} \qquad (14)$$

where τ_p denotes the local value of the mean longitudinal Reynolds stress at a vertical distance from the bed equal to $d_p/2$, and ξ is a coefficient that may be assumed to be constant for the sake of simplicity. This coefficient is expected to be much larger than unity, mainly because the entrainment is associated with absolute values of the instantaneous Reynolds stress that are much larger than τ_p. Niño & Musalem (2000) have observed that sediment entrainment is associated with instantaneous values of the Reynolds stress as large as about 5–10 times τ_p. Based on these observations, ξ is expected to have values of the order of 10.

The local value of the shear stress τ_p is related to the value of this variable at the bed through the parameter: $\phi = \tau_p/(\rho\ u^{*2})$. Replacing ϕ in Eq. 14, and then the resulting expression for u_e in Eq. 13 yields:

$$u^*/w_s = (1/\xi)\phi^{-1/2} \qquad (15)$$

To estimate ϕ, an eddy viscosity model is introduced, such that the shear stress at a distance y from the bed can be estimated as (Nezu & Nakagawa, 1993; O'Connor, 1995):

$$\tau(y) = \rho v_t u^{*2}(1 - y/h)/(v + v_t) \qquad (16)$$

Evaluating this expression at $y = d_p/2$ gives:

$$\phi = (v_t/v)/(1 + v_t/v)\,(1 - (Re^*_p/2)/Re^*_h) \quad (17)$$

where $Re^*_h = u^*h/v$, and v_t denotes the eddy kinematic viscosity at a distance from the bed equal to $d_p/2$. The ratio v_t/v is estimated according to the model proposed by O'Connor (1995), which is valid in the outer region as well as in the inner region, all across the viscous sublayer of the flow:

$$v_t/v = \kappa(Re^*_p/2)^3/[\Gamma_0^3 + Re^*_p/2)^2] \quad (18)$$

where κ is von Karman's constant with a value of 0·4 and Γ_o is a constant equal to 7·4.

Replacing Eqs 17 and 18 in Eq. 15 yields:

$$u^*/w_s = (1/\xi)(8/\kappa)^{1/2} Re^{*-3/2}_p(\Gamma_0^3 + Re^{*2}_p/4 + \kappa Re^{*3}_p/8)^{1/2}/(1-(Re^*_p/2)/Re^*_h)^{1/2} \quad (19)$$

which provides an equation to estimate the conditions for entrainment as a function of the particle Reynolds number and the flow Reynolds number Re^*_h. A comparison of this relationship with the present experimental data (Fig. 6), for different values of Re^*_h shows that a value of $\xi = 10$ provides the best fit of Eq. 19 to the experimental results.

The effect of Re^*_h on the threshold conditions for entrainment is negligible in the range $Re_p^* < 20$ for values of $Re^*_h > 100$, and this range extends to $Re_p^* < 1000$ if Re^*_h is >5000. The present model does seem to capture the observed variation in the threshold of entrainment within the viscous sublayer, although it tends slightly to overestimate the threshold value of u^*/w_s in the range $1 < Re_p^* < 5$. In order to compare the model predictions in van Rijn's parameter space (Fig. 4), the pair (u^*/w_s, Re_p^*) of Eq. 19 was transformed into the pair (u^*/w_s, R_p) using Eqs 3, 5 and 6. The resulting relationship, evaluated for a value $\xi = 10$ (as in Fig. 6), is plotted in Fig. 7, together with a curve fitted to the experimental data of Fig. 4. In the range $R_p < 20$, this curve is given by:

$$u^*/w_s = 15R_p^{-1\cdot2} \quad (20)$$

A very good agreement between Eqs 19 and 20 is observed, which validates the model proposed here at least for values of R_p lower than about 50, which is the range covered by the present experimental study.

These results support the argument that particle entrainment within the viscous sublayer is caused by intermittent turbulent activity associated with large values of the instantaneous turbulent stress that are much larger than the local Reynolds stress. The capacity of the flow to entrain particles from the viscous sublayer decays as the particles become more immersed within the viscous sublayer, at a rate similar to that of the decay of the Reynolds stress as the bottom wall is approached within the viscous sublayer.

HIDING EFFECTS: ENTRAINMENT FROM A TRANSITIONALLY ROUGH BED

No particles of sizes smaller than 112 μm were entrained in the experiments with the transitionally rough flows for the present range of shear stresses (Fig. 2). In those cases, the particles were

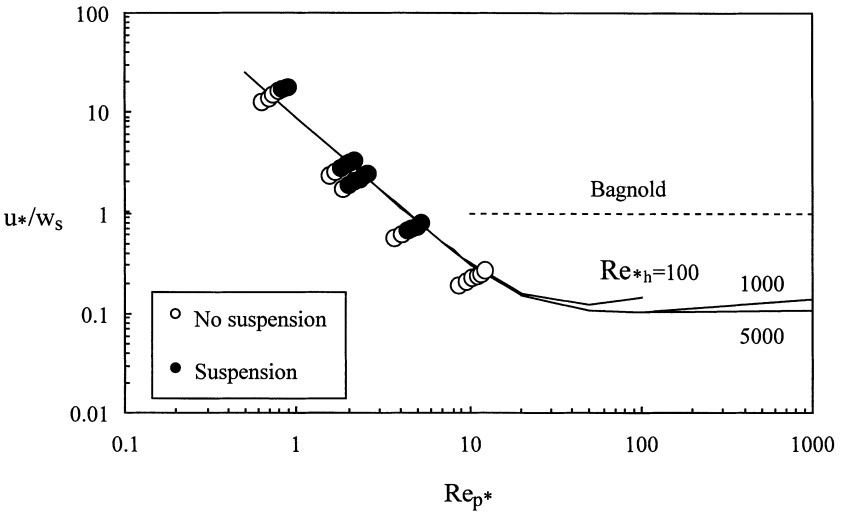

Fig. 6. Comparison between experimental results of Series S and theoretical predictions based on a bursting lift force. Solid lines represent the theoretical predictions corresponding to different Re^*_h values. Bagnold's entrainment criterion is also plotted as a reference.

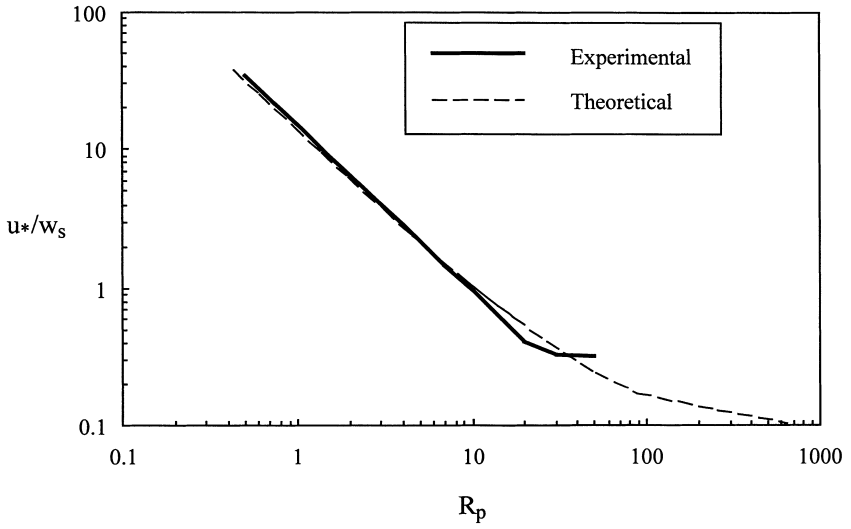

Fig. 7. Comparison between the experimental threshold of entrainment curve corresponding to Series S and theoretical predictions based on a bursting lift force. Note that for the range of R_p values plotted, the effect of Re^*_h on the theoretical prediction is negligible.

small enough to move within the interstices of the bed roughness elements from where they could not be taken away by the turbulence of the flow. In other words, the bed roughness elements seem to contribute to a hiding effect that precludes particle entrainment by locally affecting the turbulence structure of the flow.

In Fig. 8, the results from Series S and T, already presented in Figs 1 and 2, are plotted together for comparison. The threshold curve defining conditions for the initiation of suspension in Series T is displaced towards higher values of τ^* with respect to that corresponding to Series S. This implies that, as the bed roughness increased (from smooth to transitionally rough), higher values of the dimensionless shear stress were required to entrain particles of the same size, which appears to be related to the hiding effect discussed in the previous paragraph.

In Figs 1, 2 and 8, experimental points corresponding to the same particle diameter, that is to the same value of R_p, define straight lines given by Eq. 3. These lines in Figs 2 and 8 (experiments from Series T) also correspond to the same values of the ratio d_p/d_b. As this ratio becomes smaller, higher values of τ^* are needed to entrain a given particle, compared with those needed to entrain the same particle from a smooth bed (Fig. 8).

To analyse this hiding effect, the ratio between the suspension threshold value of τ^* corresponding to a particle of size d_p entrained from a bed of roughness d_b and that corresponding to a particle of the same size d_p entrained from a smooth bed, τ^*_r/τ^*_s, is plotted in Fig. 9 as a function of the ratio d_p/d_b. This is done by working directly with

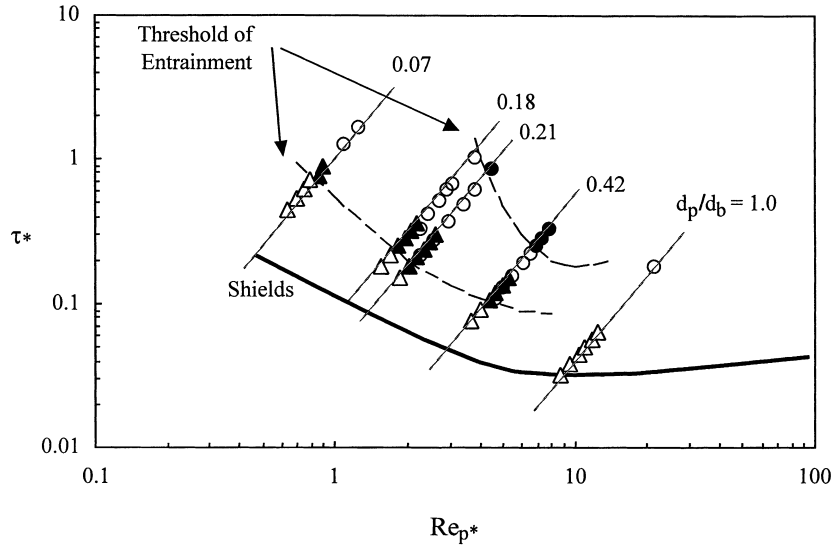

Fig. 8. Threshold of entrainment into suspension. Experimental results of Series S and T plotted together. Circles represent experiments from Series T, and triangles represent experiments from Series S. Clear circles and triangles denote experimental conditions at which no entrainment was observed. Black circles and triangles denote experimental conditions at which entrainment was observed. The dashed lines represent the threshold of entrainment. Note that the experimental points align themselves along lines of equal R_p values or, equivalently, equal d_p/d_b values. Shields' curve is also plotted as a reference.

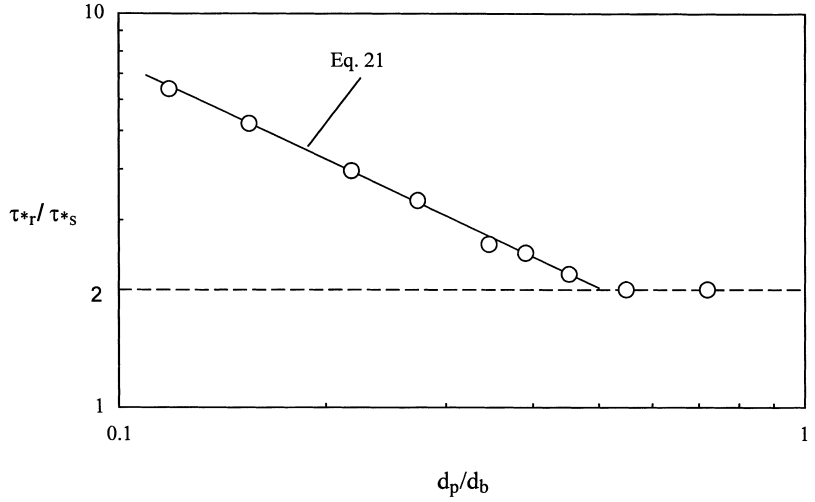

Fig. 9. Ratio between dimensionless shear stresses associated with the threshold of entrainment of a particle of size d_p entrained from a bed of roughness d_b, and the same particle entrained from a smooth bed, plotted as a function of the d_p/d_b ratio. Circles represent values obtained from the analysis of the experimental threshold of entrainment curves in Fig. 8, the solid line corresponds to a power law fit given by Eq. 21. The dashed line is plotted as a reference and shows that, for values of $d_p/d_b > 0{\cdot}5$, $\tau^*_r/\tau^*_s \approx 2$.

the threshold curves and not with the individual experimental points. For values of d_p/d_b larger than about 0·5, the ratio τ^*_r/τ^*_s has an almost constant value of about 2·0. For lower values of this parameter, τ^*_r/τ^*_s tends to increase as d_p/d_b decreases. A power law was fitted to the data, and the following relation was obtained:

$$\tau^*_r/\tau*_s = 1{\cdot}1(d_p/d_b)^{-0{\cdot}82}; \quad d_p/d_b < 0{\cdot}5 \qquad (21)$$

Remarkably, Eq. 21 resembles an equivalent equation proposed by Parker (1990) to estimate the effect of hiding in the limit conditions for the initiation of particle motion, which can be written in the form:

$$\tau^*_i/\tau*_b = (d_i/d_b)^{-\beta} \qquad (22)$$

where τ^*_i denotes the threshold dimensionless bed shear stress for the initiation of motion of a particle of size d_i lying on a surface layer formed by particles of size d_b, which have an associated threshold dimensionless bed shear stress τ^*_b. A theoretical evaluation of the exponent β, based on the concept of equal mobility, gives a value equal to 1 (Parker *et al.*, 1982); however, field evaluations of this parameter give values in the range from 0·65 to 0·9 (Parker, 1990). An excellent summary of some other relations equivalent to Eq. 22 is given by Buffington & Montgomery (1997), with the most recent of these relations being that of Wathen *et al.* (1995).

The resemblance between Eqs 21 and 22 indicates that the same physical principle is operating with regard to the hiding effect in both cases, the initiation of bedload motion and the initiation of suspension. The experimental evidence of Niño & García (1996) shows that the entrainment of particles into suspension is related to the existence of turbulent ejection events. The roughness elements of the bed induce a shielding action over the smaller particles, which tends to preclude their lifting. It is possible to speculate, based on evidence and arguments given by Wallace *et al.* (1972), Raupach (1981) and Raupach *et al.* (1991), that a less local phenomenon could also be operating. This is related to the modification of the near-bed turbulent structure of the flow, and also of the relative frequency of occurrence of sweeps and ejections, resulting from the presence of roughness elements, with respect to the case of a smooth wall.

CRITERION FOR PARTICLE ENTRAINMENT INTO SUSPENSION

The results shown in Fig. 9 suggest that, in the range $0{\cdot}5 \leq d_p/d_b \leq 1{\cdot}0$, the ratio τ^*_r/τ^*_s has a value of about 2·0. This means that a particle moving on a smooth bed is more prone to be entrained into suspension than the same particle moving on a bed formed by particles of similar size. This overexposure effect is well known in the case of initiation of motion from gravel beds (Parker, 1990), and is implicitly accounted for in Eq. 22 for values of d_i/d_b larger than unity. Overexposed particles are subjected to lesser resistance forces from surrounding smaller grains in the bed than when they are in a more homogeneous bed, surrounded by grains of similar size, which results in reduced threshold shear stress values for the overexposed particles.

Bedload particles that are entrained from a bed of smaller perched grains, as a response to larger net fluid drag forces than those acting over the smaller grains, have been called 'overpassing' grains (e.g. Everts, 1973; Allen, 1983; Carling, 1990). This overpassing phenomenon is thus closely related to the overexposure effect observed in the present experiments and refers to the same mechanisms of sediment transport.

Taking into account the previous discussion, the threshold values of τ^* for the initiation of suspension corresponding to a situation such as van Rijn's (1984) experiments, should be in the order of about twice those obtained here for Series S. Similarly, in terms of the ratio u^*/w_s, the limit of suspension corresponding to a situation such as van Rijn's should be in the order of about $\sqrt{2}$ times those corresponding to Series S.

In order to compare the present results with van Rijn's (1984) under the same conditions of particle entrainment from a bed formed by similar particles, the present threshold values of the ratio u^*/w_s were corrected, multiplying them by a factor of $\sqrt{2}$. The results obtained show that, in the range of values of R_p from 10 to 50, the corrected limit values of u^*/w_s tend to locate slightly above those of van Rijn. For values of R_p lower than about 10, the corrected limit values of u^*/w_s are much larger than those of van Rijn, and define a completely different tendency (Fig. 10). Based on the present results and using van Rijn's to extrapolate the observed tendencies towards higher values of R_p, the following threshold condition for the initiation of suspension is proposed:

$$u^*/w_s = \begin{cases} 21{\cdot}2\ R_p^{-1{\cdot}2} & 1 \leq R_p \leq 27{\cdot}3 \\ 0{\cdot}4 & R_p \geq 27{\cdot}3 \end{cases} \qquad (23)$$

Eq. 23 preserves the limit value $u^*/w_s = 0{\cdot}4$ given by Eq. 8 in the range of values of R_p larger than about 30 and improves the performance of that equation for lower values of R_p according to the present experimental results (Fig. 10).

The limit value $R_p = 27{\cdot}3$ for which the change of the exponent from −1·2 to 0 occurs in Eq. 23 corresponds to a value of Re_p^* of about 8. That is, it corresponds to particles with a size comparable to the thickness of the viscous sublayer of the flow. This means that grains that are completely immersed within the viscous sublayer behave differently from those protruding over the viscous sublayer, in that they require exponentially higher turbulent intensities to become entrained into suspension.

DISCUSSION

The present results have obvious limitations that need to be considered in an attempt to generalize them. In particular, the experimental conditions of Series T correspond to the entrainment into suspension of fine particles from a coarser bed without bedload transport. According to flow visualizations made in a related study, the presence of bedload does not seem to have a major effect on the turbulent events responsible for the ejection of particles from the bed, at least for moderate to low concentrations of particles in the saltation layer (Niño, 1995). However, detailed measurements of fluid and bedload particle

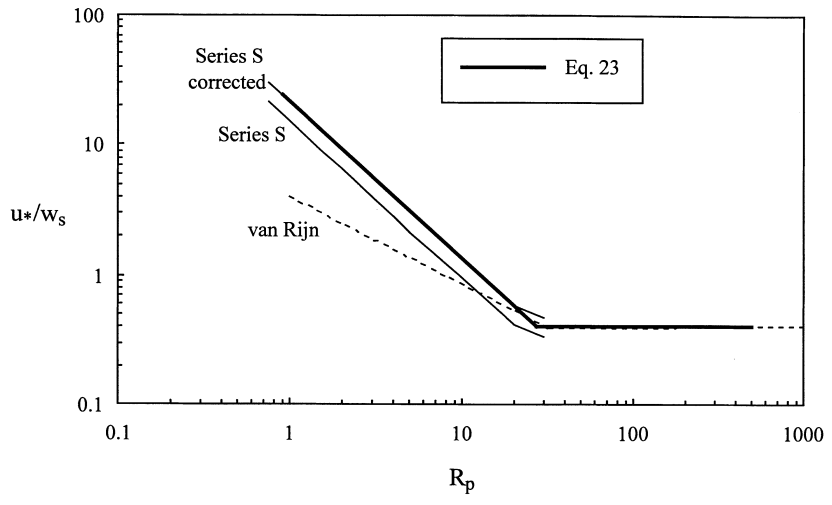

Fig. 10. Experimental threshold of entrainment of Series S corrected to represent the threshold of entrainment of particles from a bed of similar particles. The proposed criterion of entrainment given by Eq. 23 is plotted as the solid thick line together with van Rijn's (dashed line). The proposed criterion uses the present experimental results in the range R_p lower than about 30 and van Rijn's criterion for higher values of this parameter.

velocities over a fixed flat bed covered by similar particles have shown that the presence of bedload generates turbulence enhancement in the near-bed region, at least for particles of sizes comparable to the larger grains used in the present study (Best *et al.*, 1997). With bedload, increments up to about 20% in the turbulence intensities of the vertical component of the fluid velocity with respect to those in an equivalent clearwater flow, have been reported by Best *et al.* (1997). Boundary layer turbulence modification by the presence of moving particles in the near-bed region has also been reported by several other researchers (e.g. Rashidi *et al.*, 1990; Kaftori *et al.*, 1995a,b). This evidence suggests that the conditions for particle entrainment into suspension would also be affected by the presence of bedload because, as has been shown in the present paper, entrainment is modulated by the turbulence characteristics of the near-bed region. In the present experiments, entrained particles moved as bedload up to the moment of entrainment. Because of this, it can be argued that boundary layer turbulence modification might have occurred as a result of the presence of particles in the near-bed region of the boundary layer, and that the entrainment threshold proposed here takes into account such an effect. The question whether the bedload motion of coarser particles in addition to the finer entrained grains would create further modification of the near-bed turbulence, changing the entrainment threshold, cannot be answered with the present database. More experimental evidence is required to elucidate this further.

Another limitation of the present results is that they do not consider the effect of bedforms on the threshold of entrainment. It is well known that bedforms induce a major modification of the near-bed boundary layer structure, even in the case of small-amplitude ripples. Boundary layer detachment and reattachment downstream from the crest of bedforms, for instance, cause strong modification of the bed shear stress structure with respect to that of a flat bed (e.g. Nelson *et al.*, 1993). Niño & Musalem (2000) analysed particle entrainment from the crestal region of sand ripples, relating entrainment events to strong ejection and sweep events, supporting mechanisms of entrainment such as those proposed in the present paper. Entrainment from the crestal region of ripples was observed to be more intense than in other regions of the bedforms, and a bypass effect was observed, in which particles entrained from the crestal region were able to flow over the separation region downstream. It can be argued that the threshold of entrainment conditions proposed in this paper is valid in the presence of bedforms such as ripples, as identical entrainment mechanisms operate in both cases. However, local values of the bed shear stress should be considered to establish local conditions of entrainment. This means, obviously, that, in the presence of bedforms, the entrainment conditions vary along the bed depending on the relative position of the bedforms.

CONCLUSIONS

High-speed video recordings of particle motion were analysed to determine the limiting conditions for the entrainment of sediment into suspension. A threshold level of the bed shear stress was defined. For values of this variable lower than the threshold, particles are not suspended by turbulent flow ejections in the near-bed region. For values of the shear stress larger than the threshold, turbulent bursts of sediment particles are lifted from the bed into the outer regions of the wall layer, which remain in suspension for distances generally longer than about 100 particle diameters.

Bagnold's (1966) criterion seems to define an upper limit for the bed shear stress at which a concentration profile of suspended sediment starts to develop and, hence, it is different from the criterion for the initiation of suspension defined previously. On the contrary, van Rijn's (1984) criterion for the threshold of entrainment is equivalent to that used in the present study. The present results for smooth wall conditions were corrected to represent the situation in which particles are entrained from a bed formed by similar particles. The corrected results were then compared with those of van Rijn (1984). For values of R_p lower than about 30, the corrected limit values of u^*/w_s are much larger than those predicted by his relation (Eq. 8 in the present paper), and define a completely different tendency. For higher values of R_p, however, the present results agree sufficiently well with those of van Rijn (1984). A new criterion for the suspension limit is proposed (Eq. 23), which nonetheless preserves the van Rijn criterion for values of R_p larger than about 30.

The present observations (Series S) indicate that particles totally immersed within the viscous sublayer can be entrained into suspension by the flow, which contradicts previous experimental results. Nevertheless, as the particle size

decreases, higher values of the bed shear stress are needed for entrainment, which seems to be a consequence of the rather abrupt drop in turbulent intensities within the viscous sublayer as the bed is approached. This is supported by the theoretical development presented in this paper, which also shows that the entrainment of particles totally immersed within the viscous sublayer is related to the occurrence of turbulent flow events of high instantaneous values of the Reynolds stress, rather than to mean flow conditions.

In the experiments in Series T, the roughness elements induce a hiding effect that tends to preclude particle entrainment into suspension. The hiding effect was measured by the ratio τ^*_r/τ^*_s, which indicates how much larger the dimensionless bed shear stress should be to entrain a particle with a given ratio d_p/d_b with respect to that needed to entrain the same particle from the smooth bed. For values of this ratio lower than about 0·5, the ratio τ^*_r/τ^*_s follows a power law (Eq. 20), which is similar to equivalent equations for estimating the effect of hiding in the limit conditions for the initiation of bedload motion.

ACKNOWLEDGEMENTS

We thank the Chilean National Fund for Science and Technology, FONDECYT (Project 1981180), the National Science Foundation (grant CTS-9210211), the Office of Naval Research (grant N00014-93-1-0044), and the donors of the Petroleum Research Fund, administered by the American Chemical Society (grant PRF 24328-G2) for supporting this research.

NOTATION

The following symbols are used in this paper:

c_D = drag coefficient;
$D^* = R_p^{2/3}$ = dimensionless diameter;
d_b = size of roughness elements;
d_i = particle diameter of fraction i;
d_p = mean diameter of entrained particle;
F_l = mean lift force over a particle lying on the bottom wall;
$Fr = U/\sqrt{(gh)}$ = Froude number;
F_t = lift force that causes particle entrainment into suspension;
g = gravitational acceleration;
h = flow depth;
k = coefficient in the model for the mean lift force F_l;
m = exponent in the model for the mean lift force F_l;
$R = (\rho_s - \rho)$ = particle submerged specific density;
$Re = U\,h/\nu$ = Reynolds number of the flow based on the mean flow velocity and the flow depth;
$Re_p = w_s\,d_p/\nu$ = Reynolds number of the particle based on the settling velocity and the particle diameter;
$Re_p^* = u^*d_p/\nu$ = Reynolds number of the particle based on the shear velocity and the particle diameter;
$R_p = \sqrt{(Rgd_p^3)}/\nu$ = dimensionless diameter;
U = flow mean velocity;
u_e = velocity scale associated with particle entrainment;
u^* = flow shear velocity;
w_s = particle settling velocity;
W_s = submerged weight of sediment particle;
y = normal distance from the bed;
β = exponent in power law for hiding effect;
$\phi = \tau_p/(\rho u^{*2})$ = dimensionless longitudinal Reynolds stress;
$\Gamma_0 = 7{\cdot}4$ = constant in O'Connor's model for the eddy kinematic viscosity;
κ = von Karman's constant;
ν = kinematic viscosity of the fluid;
ν_t = eddy kinematic viscosity at a distance from the bed equal to $d_p/2$;
ρ = fluid density;
ρ_s = particle density;
$\tau(y)$ = local value of the longitudinal Reynolds stress at a distance from the bed equal to y;
τ_p = local value of the longitudinal Reynolds stress at a distance from the bed equal to $d_p/2$;
$\tau^* = u^{*2}/(gRd_p)$ = dimensionless bed shear stress;
$\tau^*_b = u^{*2}/(gRd_b)$ = threshold dimensionless bed shear stress for the entrainment into suspension of particles of size d_b;
$\tau^*_i = u^{*2}/(gRd_i)$ = threshold dimensionless bed shear stress for the entrainment into suspension of particles of size d_i;
$\tau^*_r = u^{*2}/(gRd_p)$ = threshold dimensionless bed shear stress for the entrainment into suspension of particles of size d_p in the experiments in Series T;
$\tau^*_s = u^{*2}/(gRd_p)$ = threshold dimensionless bed shear stress for the entrainment into suspension of particles of size d_p in the experiments in Series S;
ξ = coefficient in the model for the entrainment velocity scale u_e.

REFERENCES

Allen, J.R.L. (1983) Gravel overpassing on humpback bars supplied with mixed sediments: examples from the lower Old Red Sandstone, southern Britain. *Sedimentology*, **30,** 285–294.

Bagnold, R.A. (1966) *An Approach to the Sediment Transport Problem for General Physics*. Geological Survey Professional Paper 422-I. Geological Survey, Washington, DC.

Best, J., Bennett, S., Bridge, J. and **Leeder, M.** (1997) Turbulence modulation and particle velocities over flat sand beds at low transport rate. *J. Hydraul. Eng.*, **123,** 1118–1129.

Brownlie, W.R. (1981) *Prediction of Flow Depth and Sediment Discharge in Open Channels*. Report No. KH-R-43A. Keck Laboratory, California Institute of Technology, Pasadena, California.

Buffington, J.M. and **Montgomery, D.R.** (1997) A systematic analysis of eight decades of incipient motion studies, with special reference to gravel-bedded rivers. *Water Resour. Res.*, **33,** 1993–2029.

Carling, P.A. (1990) Particle over-passing on depth-limited gravel bars. *Sedimentology*, **37,** 345–355.

DuBoys, P. (1879) Le Rhone et les rivieres a lit affouillable. *Ann. Ponts Chaussees, Series 5*, **18,** 141–195.

Engelund, F. (1965a) A criterion for the occurrence of suspended load. *La Houille Blanche*, **8,** 802.

Engelund, F. (1965b) *Turbulent Energy and Suspended Load*. Progress Report no. 10, pp. 2–9. Coastal Engineering Laboratory, Hydraulic Laboratory, Technical University of Denmark, Lyngby, Denmark.

Everts, C.H. (1973) Particle overpassing on a flat granular boundary. *J. Waterw. Harbours Div. ASCE*, **99** (WW4), 425–438.

García, M. (2000) Discussion of 'The legend of A. F. Shields' by J. M. Buffington. *J. Hydraul. Eng.*, **126,** 718–720.

García, M., López, F. and **Niño, Y.** (1995) Characterization of near-bed coherent structures in open channel flow using synchronized high-speed video and hot-film measurements. *Exps. Fluids*, **19,** 16–28.

Grass, A.J. (1970) Initial instability of fine bed sand. *J. Hydraul. Div., ASCE*, **96** (HY3), 619–632.

Grass, A.J. (1971) Structural features of turbulent flow over smooth and rough boundaries. *J. Fluid Mech.*, **50,** 233–255.

Grass, A.J. (1974) Transport of fine sand on a flat bed: turbulence and suspension mechanics. In: *Euromech 48*, pp. 33–34. Institute of Hydrodynamic and Hydraulic Engineering, Technical University of Denmark, Lyngby, Denmark.

Hall, D. (1988) Measurements of the mean force on a particle near a boundary in turbulent flow. *J. Fluid Mech.*, **187,** 451–466.

Kaftori, D., Hetsroni, G. and **Benerjee, S.** (1995a) Particle behavior in the turbulent boundary layer. I. Motion, deposition, and entrainment. *Phys. Fluids*, **7,** 1095–1106.

Kaftori, D., Hetsroni, G. and **Benerjee, S.** (1995b) Particle behavior in the turbulent boundary layer. II. Velocity and distribution profiles. *Phys. Fluids*, **7,** 1107–1121.

Lavelle, J.W. and **Mofjeld, H.O.** (1987) Do critical stresses for incipient motion and erosion really exist? *J. Hydraul. Eng.*, **113,** 370–385.

Leighton, D. and **Acrivos, A.** (1985) The lift on a small sphere touching a plane wall in the presence of simple shear flow. *Math. Phys. Z. Angew.*, **36,** 174–178.

Liu, Z., Landreth, C.C., Adrian, R.J. and **Hanratty, T.J.** (1991) Measurements in turbulent channel flow by high resolution particle image velocimetry. *Exps. Fluids*, **10,** 301–312.

López, F. and **García, M.** (2001) Risk of sediment erosion and suspension in turbulent flows. *J. Hydraul. Eng.*, **127,** 231–235.

Mollinger, A.M. and **Nieuwstadt, F.T.M.** (1996) Measurement of the lift force on a particle fixed to the wall in the viscous sublayer of a fully developed turbulent boundary layer. *J. Fluid Mech.*, **316,** 285–306.

Nakagawa, H. and **Nezu, I.** (1981) Structure of space–time correlations of bursting phenomena in an open-channel flow. *J. Fluid Mech.*, **104,** 1–43.

Nelson, J.M., McLean, S.R. and **Wolfe, S.R.** (1993) Mean flow and turbulence fields over two-dimensional bedforms. *Water Resour. Res.*, **29,** 3935–3953.

Nezu, I. and **Nakagawa, H.** (1993) *Turbulence in Open-Channel Flows*. IAHR Monograph. A.A. Balkema, Rotterdam.

Niño, Y. (1995) Particle Motion in the Near Bed Region of a Turbulent Open Channel Flow: Implications for Bedload Transport by Saltation and Sediment Entrainment into Suspension. PhD Thesis, University of Illinois at Urbana-Champaign, Urbana, IL.

Niño, Y. and **García, M.H.** (1996) Experiments on particle–turbulent interactions in the near wall region of an open channel flow: implications for sediment transport. *J. Fluid Mech.*, **326,** 285–319.

Niño, Y. and **García, M.H.** (1998a) Engelund's analysis of turbulent energy and suspended load. *J. Eng. Mech.*, **124,** 480–483.

Niño, Y. and **García, M.H.** (1998b) Experiments on saltation of sand in water. *J. Hydraul. Eng.*, **124,** 1014–1025.

Niño, Y. and **Musalem, R.** (2000) Turbulent entrainment events of sediment grains over bedforms. In: *Fourteenth Engineering Mechanics Conference*. ASCE, Austin, TX.

O'Connor, D.J. (1995) Inner region of smooth pipes and open channels. *J. Hydraul. Eng.*, **121,** 555–560.

Parker, G. (1990) Surface-based bedload transport relation for gravel bed rivers. *J. Hydraul. Res.*, **28,** 417–436.

Parker, G., Klingeman, P.C. and **McLean, D.G.** (1982) Bedload and size distribution in paved gravel bed streams. *J. Hydraul. Div., ASCE*, **108** (HY4), 544–571.

Perry, A.E. and **Li, J.D.** (1990) Experimental support for the attached-eddy hypothesis in zero-pressure–gradient turbulent boundary layers. *J. Fluid Mech.*, **218,** 405–438.

Rashidi, M., Hetsroni, G. and **Banerjee, S.** (1990) Particle–turbulence interaction in a boundary layer. *Int. J. Multiphase Flow*, **16,** 935–949.

Raudkivi, A.J. (1990) *Loose Boundary Hydraulics*. 3rd edn. Pergamon Press, New York.

Raupach, M.R. (1981) Conditional statistics of Reynolds stress in rough-wall and smooth-wall turbulent boundary layers. *J. Fluid Mech.*, **108,** 363–382.

Raupach, M.R., Antonia, R.A. and **Rajagopalan, S.** (1991) Rough–wall turbulent boundary layers. *Appl. Mech. Rev.*, **44,** 1.

van Rijn, L.C. (1984) Sediment transport, Part II: suspended load transport. *J. Hydraul. Eng.*, **110,** 1613–1641.

Robinson, S.K. (1991) Coherent motions in the turbulent boundary layer. *Annu. Rev. Fluid Mech.*, **23,** 601–639.

Saffman, P.G. (1965) The lift on a small sphere in a slow shear flow. *J. Fluid Mech.*, **22,** 385–400 (and Corrigendum (1968), **31,** 624).

Shields, A. (1936) Anwendung der Ähnlichkeitsmechanik und der Turbulenzforschung auf die Geschiebebewegung.

Mitteilungen der Preussischen Versuchsanstalt für Wasswerbau und Schiffbau 26, Berlin, Germany.

Sumer, B.M. and **Oguz, B.** (1978) Particle motions near the bottom in turbulent flow in an open channel. *J. Fluid Mech.*, **86,** 109–127.

Sutherland, A.J. (1967) Proposed mechanism for sediment entrainment by turbulent flows. *J. Geophys. Res.*, **72,** 191–198.

Urushihara, T., Mainhart, C.D. and **Adrian, R.J.** (1993) Investigation of the logarithmic layer in pipe flow using particle image velocimetry. In: *Near-Wall Turbulent Flows* (Eds R.M.C. So, C.G. Speziale and B.E. Launder). pp. 433–446. Elsevier, Amsterdam.

Wallace, J.M., Eckelmann, H. and **Brodkey, R.S.** (1972) The wall region in turbulent shear flow. *J. Fluid Mech.*, **54,** 39–48.

Wathen, S.J., Ferguson, R.I., Hoey, T.B. and **Werritty, A.** (1995) Unequal mobility of gravel and sand in weakly bimodal river sediments. *Water Resour. Res.*, **31,** 2087–2096.

Williams, J.J., Butterfield, G.R. and **Clark, D.G.** (1994) Aerodynamic entrainment threshold: effects of boundary layer flow conditions. *Sedimentology*, **41,** 309–328.

Yen, B.C. (1992) Sediment fall velocity in oscillating flow. *Water Resour.* and Environ. Eng. Res. Report no. 11. Department of Civil Engineering. University of Virginia.

Yung, B.P.K., Merry, H. and **Bott, T.R.** (1988) The role of turbulent bursts in particle re–entrainment in aqueous systems. *Chem. Eng. Sci.*, **44,** 873–882.

Manuscript received 21 December 2000;
revision accepted 18 November 2002.